Gene Expression Signature of Human Cancer Cell Lines Treated with the Ras Inhibitor Salirasib (*S*-Farnesylthiosalicylic Acid)

Roy Blum,[1] Ran Elkon,[2] Shira Yaari,[1] Adi Zundelevich,[1] Jasmine Jacob-Hirsch,[3] Gideon Rechavi,[1,3] Ron Shamir,[4] and Yoel Kloog[1]

[1]Department of Neurobiochemistry, George S. Wise Faculty of Life Sciences, [2]David and Inez Myers Laboratory for Genetic Research, Department of Human Genetics, Sackler Faculty of Medicine, [3]Sheba Cancer Research Center and Department of Pediatric Hematology-Oncology, Safra Children's Hospital, Sheba Medical Center and Sackler Faculty of Medicine, and [4]School of Computer Science, Tel Aviv University, Tel Aviv, Israel

Abstract

Deregulation of Ras pathways results in complex abnormalities of multiple signaling cascades that contribute to human malignancies. Ras is therefore considered an appropriate target for cancer therapy. In light of the complexity of the deregulated Ras pathway, it is important to decipher at the molecular level the response of cancer cells to Ras inhibitors that would reregulate it. In the present study, we used gene expression profiling as a robust method for the global dissection of gene expression alterations that resulted from treatment with the Ras inhibitor *S*-farnesylthiosalicylic acid (FTS; salirasib). Use of a ranking-based procedure, combined with functional analysis and promoter sequence analysis, enabled us to decipher the common and most prominent patterns of the transcriptional response of five different human cancer cell lines to FTS. Remarkably, the analysis identified a distinctive core transcriptional response to FTS that was common to all cancer cell lines tested. This signature fits well to a recently described deregulated Ras pathway signature that predicted sensitivity to FTS. Taken together, these studies provide strong support for the conclusion that FTS specifically reregulates defective Ras pathways in human tumor cells. Ras pathway reregulation by FTS was manifested by repression of E2F-regulated and NF-Y–regulated genes and of the transcription factor FOS (all of which control cell proliferation), repression of survivin expression (which blocks apoptosis), and induction of activating transcription factor–regulated and Bach2-regulated genes (which participate in translation and stress responses). Our results suggest that cancer patients with deregulated Ras pathway tumors might benefit from FTS treatment. [Cancer Res 2007;67(7):3320–8]

Introduction

Ras and its effectors regulate cell growth, differentiation, motility, survival, and death (1). Deregulation of Ras pathways by mutational activation or by receptor-mediated activation of Ras contribute to human malignancies (1). Approximately one third of all human cancers, including cancers of the pancreas, colon, and lung, express a constitutively active oncogenic Ras (1). Therefore, inhibition of Ras or its upstream activators or downstream effectors seems to be a promising pharmacologic strategy for cancer therapy (2, 3). Several such inhibitors are indeed already in clinical use, and a significant number of new inhibitors are at various stages of clinical trials (3). One such compound is the Ras inhibitor *S*-farnesylthiosalicylic acid (FTS; salirasib), which interferes with Ras membrane anchorage (3, 4). FTS was shown to efficiently inhibit the active GTP-bound Ras in various human cancer cell lines (3, 4). Treatment of cancer cells with FTS results in diminished Ras signaling and attenuation of cell growth *in vitro* and *in vivo* (4–8). Those early experiments suggested that deregulated Ras pathways could apparently be "corrected," at least in part, by FTS. This notion was supported by the close positive correlation recently observed between the probability of Ras pathway deregulation determined by gene expression profiling and the extent of inhibition of cell proliferation by FTS (9).

These and related studies (10, 11) emphasized the usefulness of genetic profiling in defining Ras and other oncogene pathway deregulation signatures in cancer cells. Such profiling is particularly important for the design of drug treatments because cancer cells exhibit a plethora of genetic aberrations, many of which, like the chronically active Ras, participate in the deregulated growth and in cell death (12). Here, we used the robust method of high-throughput microarray expression profiling combined with advanced bioinformatic tools (13) to analyze the response of a variety of human cancer cells to FTS. We established a comprehensive database of five different FTS-treated human tumor cell lines that exhibit diverse abnormalities in Ras and in Ras-related signaling pathways. The cell lines examined in this study were U87 glioblastoma cells characterized by large amounts of activated wild-type Ras reflecting overexpression of tyrosine kinase receptors, A549 non–small cell lung carcinoma (NSCLC) cells with constitutively active oncogenic K-Ras(12V), LAN1 neuroblastoma cells with amplified *Myc-N* gene, SHEP neuroblastoma cells devoid of amplified *Myc-N* gene, and NCIH929 myeloid cells that harbor oncogenic N-Ras(13V) and amplified *c-Myc* gene. We then applied an integrative analysis of gene expression profiles to search for FTS-induced core transcriptional responses that are shared by all of the tested cell lines.

Materials and Methods

Cell culture. The human tumor cell lines used and their growth conditions have been described previously (5, 6). FTS was a gift from Concordia Pharmaceuticals (Sunrise, FL). Cell proliferation assays and determination of IC_{50} values (FTS concentration that induces 50% growth inhibition) were done as described (5, 6). The effect of FTS on gene

Note: Supplementary data for this article are available at Cancer Research Online (http://cancerres.aacrjournals.org/).

Y. Kloog is the incumbent of The Jack H. Skirball Chair for Applied Neurobiology. G. Rechavi is the incumbent of the Djerassi Chair in Oncology. R. Shamir is the incumbent of the Raymond and Beverly Sackler Chair in Bioinformatics.

Requests for reprints: Yoel Kloog, Department of Neurobiochemistry, George S. Wise Faculty of Life Sciences, Tel Aviv University, 69978 Tel Aviv, Israel. Phone: 972-3-640-9699; Fax: 972-3-640-7643; E-mail: kloog@post.tau.ac.il.

doi:10.1158/0008-5472.CAN-06-4287

expression in various cell lines was determined 24 and 48 h or 72 h after treatment with FTS or vehicle (Fig. 1*A*) as described (5, 6). Zero-time incubation was included. Total RNA from each sample was used to prepare fragmented cRNA for hybridization (5, 6).

Analysis of gene expression data. For gene expression profiling of each tumor cell line, done by comparing samples from FTS-treated cells and vehicle-treated control cells at the time points and drug doses listed in Fig. 1*A*, we used Affymetrix (Santa Clara, CA) Human Genome Focus oligonucleotide arrays representing more than 8K well-annotated genes that collectively cover all aspects of cellular physiology. Data on U87 and LAN1 cells were taken from our earlier studies (5, 6), and data on SHEP, A549, and NCIH929 were generated here.

First, we filtered the probe sets of all five cell lines, representing 11 different conditions (Fig. 1*A*), to generate expression profiles that were detectable by the Affymetrix MAS 5 analysis package as "present" in at least one sample and whose expression was flagged as "increased" or "decreased" under at least one FTS-treated condition. This filtration procedure generated a list of 5,111 probe sets (see Supplementary Table S1). We then subjected the gene expression data under the 11 conditions to hierarchical clustering using the EXPANDER software (14). Before clustering, the expression levels of each gene were standardized so that mean is equal to 0 and variance is equal to 1.

To define a set of genes that responded to FTS treatment, we applied a rank-sorting method for selecting the most reactive genes that were changed in the same direction in most of the conditions. For each condition, all 5,111 probes sets were sorted according to the magnitude of their log ratio values. We then calculated the average rank of each gene and selected the 500 genes with the highest average rank and the 500 genes with the lowest average rank (a total of 1,000 active genes; see Supplementary Table S2). To identify the major expression patterns, we subjected these responsive genes to cluster analysis using the CLICK algorithm (15) implemented in the EXPANDER package.[5] After standardization, positive and negative values no longer represented up-regulation and down-regulation; therefore, for visualization purposes, we added to the data a dummy condition (column) representing "no change." The dummy condition allows the visual distinction between absolute up-regulation and down-regulation. Standardized log ratio values above and below the standardized dummy level then represented up-regulation and down-regulation, respectively.

Analysis of functional categories. Software for association of human genes with the Gene Ontology category of biological processes was downloaded from the Gene Ontology Web site.[6] Enrichments of specific clusters for genes of a particular functional category were identified using the TANGO algorithm implemented in EXPANDER, in which hypergeometric calculation is used to determine overrepresented Gene Ontology functional categories in a target set relative to a background set. The group of genes of interest was used as the target set, whereas the background set comprised the 5,111 probe sets. Certain genes were represented in the microarray by several probe sets. To avoid biases, genes represented by multiple probe sets were counted only once.

Computational promoter analysis. We applied the PRIMA algorithm (13) implemented in EXPANDER to identify *cis*-regulatory promoter elements that control the observed transcriptional modulation in our microarray data set. Given target and background sets of promoters, PRIMA does statistical tests to identify transcription factors whose binding site signatures are significantly overrepresented in the target set relative to background (transcription factor enrichment is indicated by *P* value).

Real-time PCR analysis. Extracts of total RNA (1 μg) from U87 cells treated for 48 h or A549 cells treated for 72 h with FTS (75 μmol/L) or vehicle (control) were reverse transcribed using the iScript cDNA kit (Bio-Rad Laboratories, Hercules, CA) as described (16). The cDNA samples were used for real-time PCR (SYBR Green PCR kit, Roche Diagnostics, Mannheim, Germany) as described (16) using the primers 5-AAGAACGAGAAGCAG-CATTTG-3 and 5-TTCTGAGCCCGGACAATACA-3 [activating transcription factor (ATF) 3] or 5-ATGATTACCTGGAGGTGG-3 and 5-ATCC-TCCTTGCTGTTGTTGG-3 (ATF4) or primers for the housekeeping gene *HMBS* (5).

A

Condition*	Cell line	Treatment	IC50 (μmol/L)
1	U87	75μmol/L, 24h	50
2	U87	75μmol/L, 48h	
3	A549	75μmol/L, 24h	40
4	A549	75μmol/L, 48h	
5	A549	75μmol/L, 72h	
6	LAN1	75μmol/L, 24h	35
7	LAN1	75μmol/L, 48h	
8	SHEP	75μmol/L, 24h	50
9	SHEP	75μmol/L, 48h	
10	NCIH929	50μmol/L, 72h	60
11	NCIH929	75μmol/L, 72h	

*Each condition refers to paired samples of the vehicle control and the drug treated cells.

B

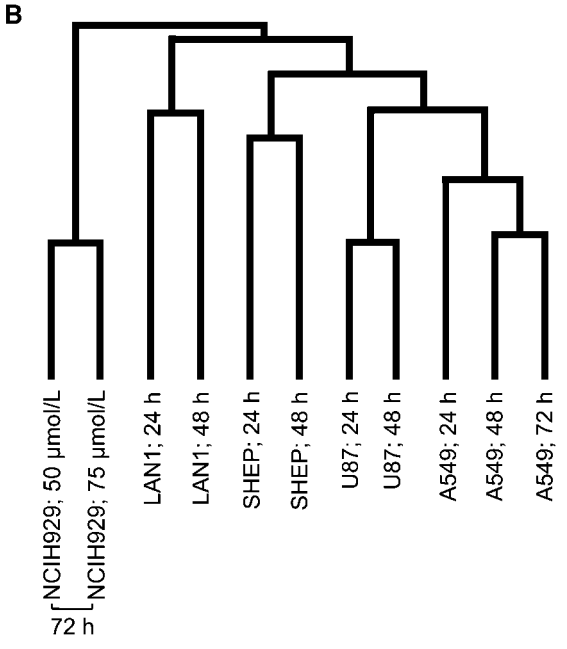

Figure 1. Cancer cell lines and hierarchical clustering analysis of the FTS-induced alterations in gene expression under the various conditions used in the study. *A,* cell lines were analyzed and treatment conditions are recorded. IC_{50} values for growth inhibition were generated from FTS growth inhibition curves as described in Materials and Methods. *B,* hierarchical clustering of the FTS-induced changes.

[5] http://www.cs.tau.ac.il/~rshamir/expander
[6] http://www.geneontology.org/doc/GO.current.annotations.html

Results

Profiling of gene expression in FTS-treated human tumor cell lines. To identify common transcriptional responses to FTS treatment, we did a global analysis of gene expression in five different FTS-treated tumor cell lines under conditions at which cell growth is inhibited. Because, under certain conditions, FTS can induce apoptotic cell death (5, 6), gene expression analysis was done in each cell line according to its sensitivity to FTS under defined conditions at which cell growth was inhibited but the cells do not die. The IC_{50} values for FTS-induced inhibition of cell growth (Fig. 1*A*) are relatively high because FTS binds to the serum proteins, and this leads to low free drug concentrations in the growth medium (4–8). In all cases, we examined two or three pairs of cell preparations that included the vehicle control and the drug-treated cells at one or two concentrations or a single dose at two or three time points. Altogether, 22 samples of RNA extracts were isolated from the five sets of human tumor cell lines and subjected to Affymetrix gene expression analysis. This generated a database of FTS-induced alterations in gene expression as reflected from 11 distinct conditions (Supplementary Table S1; Fig. 1*A*), enabling us to do a global dissection of the transcriptional response to FTS.

Global hierarchical clustering analysis of FTS-treated cancer cells. Next, we subjected the data sets to hierarchical clustering of the conditions (Fig. 1*B*). This analysis yielded an appreciation of the general pattern of gene expression alterations manifested in the different cell lines. The hierarchical clustering showed that, in each case, all the conditions related to the same cell line were grouped together in one branch (Fig. 1*B*). This indicated that the microarray measurements were robust and could preserve the unique transcriptional behavior of each type of cell line. Moreover, all the conditions related to U87 and A549 cells were clustered together in a common branch, possibly reflecting a stronger dependence of these cells on Ras signaling (Fig. 1*B*). Hierarchical clustering applied to the 22 conditions (i.e., before dividing the values of treated samples by their untreated controls) yielded a primary partition of the dendrogram according to cell line/tissue and a secondary one reflecting FTS treatment (data not shown), showing that the effect of tissue of origin on expression profile is stronger than that which results in response to FTS.

Ranking-based identification of major expression patterns in FTS-treated cells. To focus on the most prominent FTS-induced alterations in gene expression, we first applied a ranked sorting method that selected the most reactive genes with changes in the same direction under most of the conditions (see Materials and Methods). The ranking-based list (Supplementary Table S2), representing the 1,000 most responsive genes (500 up-regulated and 500 down-regulated by FTS treatment), was then used for all subsequent data analysis. The response of these genes to FTS treatment in the various cell lines clearly shows the common patterns of changes in gene expression across all 11 examined conditions (Fig. 2*A*).

To further identify prominent expression patterns among the ranking-based 1,000 active genes, we subjected the data (log ratios) to cluster analysis using the CLICK algorithm implemented in the EXPANDER package (14, 15). Before clustering, the log ratios of each gene were standardized to mean equal to 0 and variance equal to 1 (15); hence, genes that are clustered together show similar alteration patterns across the tested conditions but might differ in the magnitude of their response. CLICK (15) identified two major clusters, representing decreased and increased steady-state mRNA

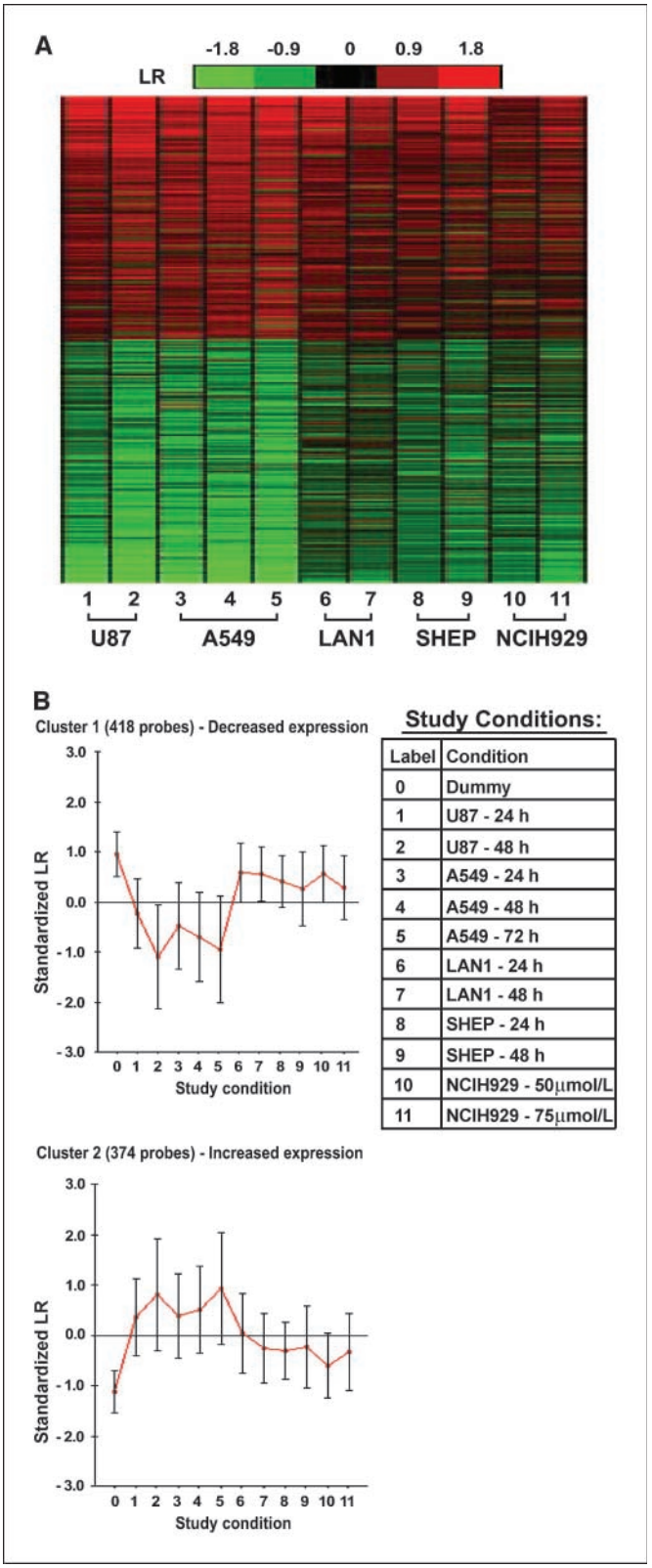

Figure 2. Ranking-based heat maps and cluster analysis by EXPANDER. *A,* heat-map images depicting a common pattern of changes in gene expression [log ratios (*LR*)] induced by FTS in all data sets (indicated in *B*). *B,* two major clusters of genes whose expression was decreased or increased by FTS treatment in all data sets. *Y axis,* standardized log ratios generated as described in Materials and Methods; *X axis,* each of the conditions (data sets) as indicated in *right. Bars,* SD.

Table 1. Overrepresented functional categories within gene clusters regulated by FTS

Cluster	No. genes associated with the category	Functional category	Gene Ontology ID	P*	Corrected P †
1	44	DNA replication	0006260	4.7×10^{-24}	<0.001
	40	Mitosis	0007067	2.1×10^{-23}	<0.001
	44	M phase	0000279	4.1×10^{-23}	<0.001
	46	Mitotic cell cycle	0000278	1.4×10^{-22}	<0.001
	76	DNA metabolism	0006259	4.0×10^{-22}	<0.001
	82	Cell cycle	0007049	4.4×10^{-19}	<0.001
	33	Cell division	0051301	3.9×10^{-16}	<0.001
	25	Microtubule-based process	0007017	4.1×10^{-14}	<0.001
	14	Spindle organization and biogenesis	0007051	8.5×10^{-14}	<0.001
	140	Biopolymer metabolism	0043283	2.1×10^{-11}	<0.001
	35	Response to DNA damage stimulus	0006974	9.3×10^{-11}	<0.001
	151	Nucleic acid metabolism	0006139	2.9×10^{-10}	<0.001
	57	Organelle organization and biogenesis	0006996	2.0×10^{-9}	<0.001
	96	Nucleotide binding	0000166	4.0×10^{-7}	0.002
	11	Cell cycle checkpoint	0000075	1.9×10^{-6}	0.002
	12	Phosphoinositide-mediated signaling	0048015	2.8×10^{-6}	0.002
	243	Primary metabolism	0044238	3.2×10^{-6}	0.002
	184	Protein binding	0005515	1.1×10^{-5}	0.008
2	11	Ligase activity/forming phosphoric ester bonds	0016886	2.2×10^{-7}	0.002
	22	Amino acid metabolism	0006520	3.3×10^{-6}	0.002
	39	Programmed cell death	0012501	6.3×10^{-6}	0.004
	17	Translation	0043037	3.5×10^{-5}	0.028
	37	Protein localization	0008104	3.8×10^{-5}	0.029

*P values were calculated using the tail of the hypergeometric distribution.
†P values were corrected for multiple testing using empirical sampling (of 1,000 random clusters; see ref. 14 for details).

levels: cluster 1 contained 418 genes whose expression was decreased by the FTS treatment and cluster 2 contained 374 genes whose expression was increased by the FTS treatment through all the condition sets (Fig. 2*B*). Inspection of these two clusters revealed that the most vigorous response to FTS treatment was shown by the U87 and A549 cell lines (Fig. 2*B*). Five smaller clusters, consisting of 20 to 50 genes, exhibited more complex patterns (data not shown) and were not analyzed further.

Identification of overrepresented functional categories within gene clusters up-regulated or down-regulated by FTS. To characterize the biological processes participating in the response to the treatment with FTS in all cancer cell lines, we used EXPANDER for statistical analyses aimed at identifying functional categories that are significantly enriched in the clusters. For description of biological processes, we used the standard Gene Ontology vocabulary. Enriched functional categories ($P \leq 0.05$, after correction for multiple testing) were identified in each of the two main clusters (Table 1; see Supplementary Table S3 for a list of the genes associated with each of the enriched functional categories).

The cluster of down-regulated genes (cluster 1) showed extremely high enrichment for genes related to mitosis, cell cycle, DNA replication, spindle organization and biogenesis, nucleotide binding, and cell cycle checkpoint categories (Table 1). For example, FTS seemed to decrease the expression of genes required for cell growth, such as cell cycle phosphatases (*CDC25A* and *CDKN3*), cell cycle kinases (*CDC2* and *CDK2*), polymerases (*POLA2* and *POLE2*), minichromosome maintenance proteins (*MCM2* and *MCM5*), cyclins (*CCNA2* and *CCNE2*), transcription factors (*E2F1* and *FOS*), and oncogenes (*RAB4A*; see Supplementary Table S3). This finding is in accordance with the FTS-induced inhibition of DNA synthesis and cell growth observed in the cancer cell lines screened here (3, 5–7). The decrease in expression of this remarkably large number of cell cycle regulatory genes, which was common to all tested cell lines, points to a fundamental core response to FTS. It is also worth noting that FTS decreased the transcript level of the antiapoptotic gene survivin in all five tested cell lines, in agreement with our recent observation in U87 cells and prostate cancer cells (16).

The up-regulated genes (cluster 2) showed high enrichment for genes related to the programmed cell death category (Table 1). Thus, FTS seemed to induce the expression of several proapoptotic genes, including *BAK1*, the tumor suppressor *TP53*, which plays a role in apoptosis and whose mRNA steady-state level was shown to be up-regulated by FTS in human colon carcinoma (8), *GADD45A*, which participates in the induction of apoptosis (17), and *FOXO3A*, which functions as a trigger for apoptosis (Supplementary Table S3). Interestingly, expression of the p21(WAF1/CIP1) cell cycle inhibitor (*CDKN1A*), previously shown to be up-regulated by FTS in human colon carcinoma (8), was also increased in all FTS-treated cancer cell lines. The observed enrichment in up-regulated apoptosis-related genes is in accord with our earlier observations that FTS can stimulate cell death mechanisms in a variety of cancer cell lines (5).

An additional category of up-regulated genes in cluster 2 was that of genes that participate in amino acid metabolism known to be associated with stress response (Table 1). Included in this group are several genes encoding aminoacyl-tRNA synthetase enzymes (Supplementary Table S3). Interestingly, Met-tRNA synthetase is

up-regulated in response to hypoxic stresses (18), raising the possibility that the response of cancer cells to FTS might involve adaptation to stress.

Only few outliers were detected in search for genes that were up-regulated or down-regulated in a counterintuitive manner. These included *CASP8AP2*, a proapoptotic gene that was down-regulated, and several genes that were up-regulated. These genes included *EREG*, an epidermal growth factor receptor ligand, *BIRC4*, which inhibits apoptosis, *IL6*, which can contribute to expression of a malignant phenotype, and *IL8*, a potent angiogenic factor.

Promoter analysis of FTS-induced down-regulated genes reveals a prominent signature of cell cycle arrest. The primary target of FTS is the active Ras protein (3, 4), whose signaling pathways control a large number of transcription factors regulating expression of genes involved in cell cycle and cell survival. We therefore did global promoter analysis to identify common transcription factors participating in the response of cancer cells to FTS. We were particularly interested in tracking regulators whose modulation in response to the drug treatment could be interpreted in light of the defined functional categories of the responding genes. To this end, we applied the promoter analysis algorithm PRIMA (13) implemented in the EXPANDER package. Each of the two gene clusters described above (Fig. 2*B*) was considered a target set, and the entire set of 5,111 genes served as the background (see Materials and Methods). In cluster 1 (FTS-induced down-regulated genes), PRIMA identified four enriched transcription factor–binding site signatures: E2F, NF-Y, ZF5, and nuclear respiratory factor-1 (NRF1; $P < 0.002$; Fig. 3*A*). Enrichment was highest for E2F and NF-Y, both well-established transcriptional regulators of the cell cycle that are controlled by Ras (19–21). Evidently, high levels of active Ras and increased activation of E2F and NF-Y are common to many human tumors (19, 21–23).

A large number of genes (74) contained at least one high-scoring putative E2F-binding site (Supplementary Table S4), among them genes known to be under the direct control of E2F, such as *CDC6, DNMT1, MCM2, MCM3, MCM5, POLA, POLE, POLE2, CDC25A*, and *DHFR*. Because all of these genes are functionally important in S phase, these results are consistent with those obtained by functional analysis showing a common signature of cell cycle arrest (Table 1). Other genes identified here are not known to be regulated by E2F and thus might represent novel putative E2F targets.

EXPANDER also identified 136 genes containing at least one high-scoring putative NF-Y–binding site, among them several that were previously reported to be positively regulated by NF-Y (e.g., *CCNA2, CCNB2, CDC25C*, and *CDC2*; refs. 24, 25). These genes are associated with mitotic cell cycle, M phase, and cell proliferation, and the expression of some of them is reportedly controlled by Ras (25, 26). Here, too, EXPANDER identified other genes that could represent novel putative NF-Y targets. EXPANDER also identified enrichment in NRF1 and ZF5.

Promoter analysis of FTS-induced up-regulated genes reveals a prominent signature of a stress response. Promoter analysis of the FTS-induced up-regulated genes (cluster 2) identified four transcription factors whose binding site signatures were overrepresented in the target set (Fig. 3*A*). These were the transcription factors Bach2, ATF, Elk-1, and FAC1. The highest enrichment was observed for Bach2. Bach2 is a transcription factor known to be regulated by an oxidative stress–sensitive conditional nuclear export.

The promoter analysis also pointed to enrichment in ATF-regulated and Elk-1–regulated genes, suggesting that FTS up-regulates their transcriptional activities. Both transcription factors are associated with stress responses (27, 28). In addition, the microarray data suggested not only an increase in ATF-regulated genes but also increases in the steady-state levels of mRNAs encoding four members of the ATF family (*ATF3, ATF4, ATF5*, and *ATF6*) themselves, which seemed to be elevated by FTS in all FTS-treated cancer cell lines. The most prominent elevations were observed in ATF3 and ATF4 (2- to 15-fold; see also Fig. 3*B*). Real-time PCR confirmed the marked increase in ATF3 and ATF4 mRNA levels in U87 and A549 cells (Fig. 3*C*).

Patterns of Ras pathway reregulation by FTS match signatures of Ras pathway deregulation and neoplastic transformation. Recent gene expression profiling identified distinctive patterns of oncogenic pathway deregulation in human mammary epithelial cells infected with adenovirus expressing activated H-Ras, c-Myc, c-Src, activated β-catenin, or E2F3 (9).

A

Cluster	TF	Accession number in TRANSFAC DB	Enrichment Factor	p-value
1	E2F	M00918	2.06	$8.6*10^{-11}$
	NF-Y	M00287	1.74	$7*10^{-16}$
	ZF5	M00716	1.16	0.001
	NRF1	M00652	1.2	0.002
2	Bach2	M00490	1.64	$4.8*10^{-5}$
	ATF	M00017	1.29	0.002
	Elk-1	M00025	1.3	0.002
	FAC1	M00456	1.33	0.002

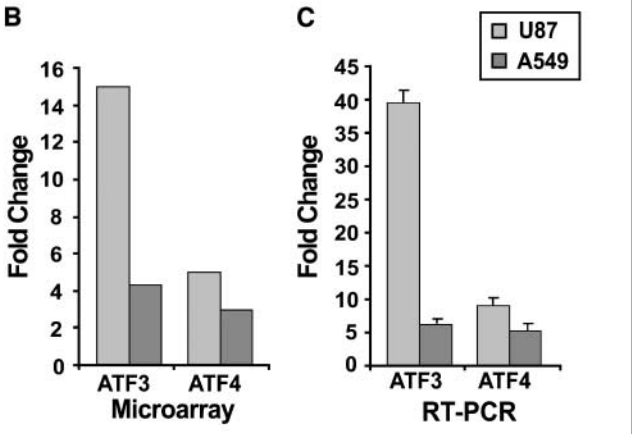

Figure 3. Promoter analysis of FTS-induced down-regulated and up-regulated genes. *A,* transcription factors (*TF*) whose binding site profiles were enriched in the two clusters described in Fig. 2. Most significant enrichments in each cluster of down-regulated genes and in each cluster of up-regulated genes. *P* values indicate the significance of transcription factor signature enrichment in the cluster relative to that in the background set as described in Materials and Methods. Enrichment factor values represent the frequency of the transcription factor signature in a cluster divided by its frequency in the background set. *B,* effects of FTS on transcription of ATF3 and ATF4. Data generated in U87 and A549 cells (see Materials and Methods) are presented as the fold change in expression of ATF3 and ATF4. *C,* real-time PCR analysis of ATF3 and ATF4 transcripts in control and FTS-treated U87 and A549 cells. Transcript levels were normalized to the expression of *HMBS* (housekeeping gene). Data are expressed as ratios of ATF3 or ATF4 values in FTS-treated cells relative to control values.

These patterns were used to develop expression signatures predictive of oncogene-specific pathway deregulation and drug sensitivity (9). In this study, we identified the gene expression signature that seems to reflect FTS-induced reregulation of Ras pathways. To examine the correspondence between our results and the oncogene deregulation signatures defined in ref. 9, we compared the lists of the 1,000 most responsive genes (the core transcriptional response to FTS; Supplementary Table S2) probed in our study and the H-Ras–, c-Myc–, c-Src–, β-catenin–, and E2F3-derived signatures. The results of the analysis (Supplementary Table S5) show that only a relatively small proportion of genes in the c-Src–derived (6%), β-catenin–derived (2%), and c-Myc–derived (4%) deregulation signatures shared commonality with genes that were altered in the cancer cell lines by the FTS treatment. A relatively high proportion of genes (8%) in the E2F3-transformed cells showed commonality with genes that were altered in the FTS-treated cancer cell lines, and the highest proportion of common genes was found in the activated H-Ras–transformed cells and FTS-treated cells (12%). Interestingly, this correspondence was even improved when the oncogene deregulation signatures were compared with the gene signature of A549 cells, which, unlike the other cell lines, express the constitutively active K-Ras(G12V) (Supplementary Table S5). Next, we compared the Ras signature with genes that were differentially expressed in NSCLC with and without Ras mutation (see Fig. 2*C* in ref. 9). Among the 248 genes that were up-regulated by FTS treatment and were differentially expressed in the NSCLC ($P < 0.05$), 153 and 95 were down-regulated and up-regulated in the Ras-mutated samples, respectively. Among the 302 genes that were down-regulated by FTS treatment and were differentially expressed in the NSCLC ($P < 0.05$), 226 and 76 were down-regulated and up-regulated in the Ras-mutated samples, respectively. Thus, both positive and negative overlaps are observed, indicting that FTS treatment and expression of oncogenic K-Ras elicit opposite responses as expected as well as common responses. The latter could be associated with general physiologic perturbations.

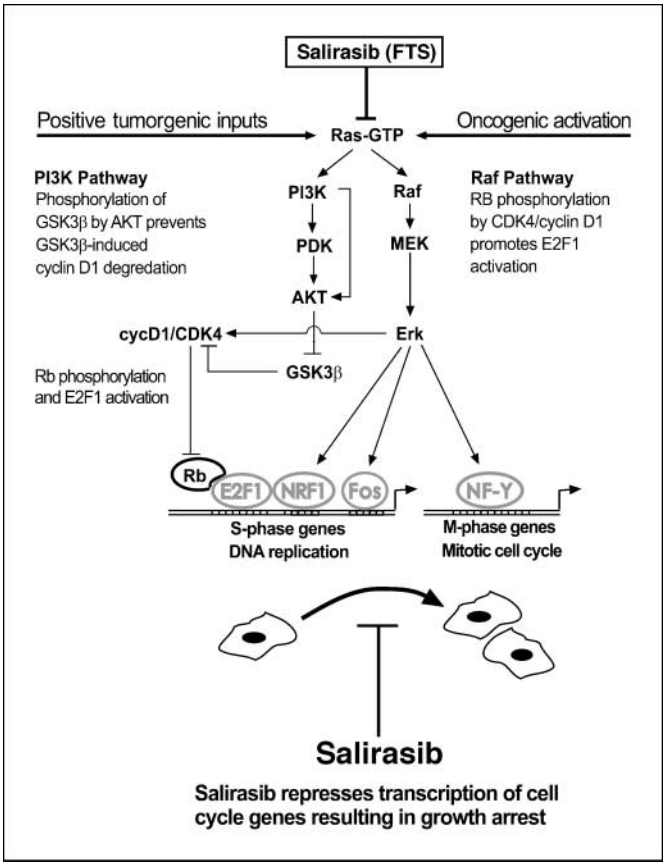

Figure 4. Proposed model for the salirasib-induced repression of cell cycle genes leading to inhibition of cancer cell growth. Ras pathways participating in regulation of cell cycle progression (19–21). Ras inhibition by FTS reduces ERK activation and cyclin D1/CDK4 assembly and increases GSK3β-mediated degradation of cyclin D1, together resulting in down-regulation of the transcription factor E2F1. Positive regulation of the transcription factors NRF1, FOS, and NFY by ERK is also diminished.

Next, we sought to examine the correspondence between the FTS-induced signature and the previously described meta-signature identifying genes that are overexpressed in most cancer types relative to the normal tissues from which they arose and that seem to reflect essential transcriptional traits of neoplastic transformation (29). We found that the FTS signature (Supplementary Table S2) fitted well to the gene meta-signatures of undifferentiated tumors (see Fig. 3 in ref. 29). Of the 69 genes of the meta-signature, there were 33 in common with the FTS signature and 27 genes in this common list (82%) were strongly down-regulated by FTS. These included the cell cycle genes (*CDC2, MCM3, CDNK3*, and *TOP2A*) and additional genes critical for malignant transformation, such as *PCNA* and *BIRC5*. We also compared the FTS signature and the distinct expression signature of glioblastoma multiformes (GBM) generated by profiling normal brain and brain tumor tissues from 32 patients (30). Of the 97 characterized genes (GBM signature) that are more highly expressed in GBMs than in normal brain (see Fig. 2 in ref. 30), we identified 67 in common with the FTS signature, of which 47 (77%) were down-regulated by FTS.

Overall, the comparative analyses showed that the FTS signature points to reregulation of the deregulated Ras pathways as well as of the transcriptional profiles that seem to be essential for neoplastic transformation (29, 30).

Discussion

A ranking-based procedure combined with functional analysis and promoter sequence analysis (31) enabled us to decipher the common and most prominent patterns of the gene expression response of five different human cancer cell lines to the Ras inhibitor FTS (salirasib). The analysis required the use of a method that allows comparisons of gene expression profiles in a manner that is less sensitive to outliers. We therefore used a ranking-based gene selection procedure in combination with functional analysis and promoter sequence analysis using the EXPANDER (14). Although this method maximizes the detection of the effects of FTS on gene expression, the genetic differences among the cell lines cannot be completely eliminated. Some differences among cell lines in response to FTS, which are not discussed here, were indeed detected. Our major aim in this study was to identify a core response to FTS, which is universally shared by all probed cell lines regardless of genetic and tissue differences.

Remarkably, the functional analysis yielded enriched Gene Ontology categories of cell cycle progression, cell death, and stress response. Similarly the PRIMA promoter analysis yielded enriched transcription factor signatures typical of regulators of the cell cycle and of stress. These complementary results established a signature of Ras pathway reregulation by FTS. The signature of the FTS treatment fitted well to a deregulated H-Ras pathway signature that

by itself predicted sensitivity to FTS (9). These experiments provided strong support for the notion that FTS specifically reregulates defective Ras pathways in human cancer cells.

Attenuation of cell division. The core transcriptional repression response to FTS is clearly attributable to the known anti-Ras activity of this inhibitor, which results in inhibition of cancer cell growth. Our analysis points to the suppression of genes that are positively regulated by the transcription factors E2F and NF-Y. These transcription factors are, respectively, essential for cell cycle progression through S phase and mitosis (25, 26). The FTS-induced suppression of genes regulated by E2F and NF-Y implies that their transcriptional activity is reduced as a consequence of Ras inhibition as presented schematically in Fig. 4. Ample evidence indeed exists for the critical role of active Ras and its downstream effectors in regulation of the cyclin-dependent kinase 4 (CDK4)-cyclin D1/RB/E2F1 pathway (32) and of NF-Y activation (21, 33). In addition, we and others have shown that, concomitantly with FTS inhibition of Ras, the levels of cyclin D1 are decreased and the activity and expression of E2F are down-regulated in various human tumor cell lines, including U87 glioblastoma cells, neuroblastoma LAN1 cells, melanoma, and LNCaP and PC3 prostate cells (3, 6). In addition, forced expression of E2F1 can overcome the growth-inhibitory effects of FTS (34).

The core transcriptional repression response to FTS includes reduction in NRF1 (Fig. 3*A*), a transcription factor known to regulate expression of genes participating in mitochondrial function and mitochondrial biogenesis (35). This observation suggests that Ras signals might positively regulate NRF1 target genes and mitochondrial functions (see scheme, Fig. 4). This possibility is supported by earlier studies showing that extracellular signal-regulated kinase (ERK) and p38 mitogen-activated protein kinase (MAPK) participate in NRF1 nuclear accumulation (36) and that NRF1 might play an integrative role in nucleo-mitochondrial interactions (35).

Interestingly, in two recent genome-wide analyses of transcription factors, motif-finding algorithms predicted the existence of NRF1-binding sites in E2F target promoters (13, 37). A genome-wide transcription factor analysis confirmed these predictions and showed that NRF1 functions as a coregulator of numerous E2F target genes (37). Thus, NRF1 plays a role as a regulator of cell cycle genes as well as of genes that participate in mitochondrial function. In line with these findings, our promoter analysis showed that many genes described as NRF1 targets are also E2F targets, suggesting common regulation of these genes by both E2F and NRF1 (13, 37). Importantly, our analysis identified 103 genes in cluster 1 whose promoters contained binding sites for NRF1 but not for E2F, suggesting that, in addition to E2F, FTS also induces down-regulation of NRF1.

Enhancement of stress response genes. The common transcriptional induction response to FTS of cancer cells seems to be associated mainly with a stress response as shown by the up-regulation of the transcription factors ATF3, ATF4, and Bach2 (Fig. 3*A*). Stress responses induced by a variety of stimuli, including amino acid starvation, endoplasmic reticulum stress, oxidants, and cytotoxic drugs, enhance transcription of ATF4 and ATF3 and reduce global translation (38, 39). Whereas global translation in the stressed cells is reduced, translation of ATF4 and ATF3 is enhanced, leading to the transcriptional transactivation of ATF3/ATF4 target genes, which in turn function toward adaptation of the cell to the stress insult by reconfiguration of gene expression (38).

The mechanisms of typical stress responses and the control of protein synthesis have been well characterized. Both stress kinases GCN2 and PERK, each of which is activated by different stress signals, directly phosphorylate the eukaryotic initiation factor eIF2α at Ser^{51}. Phosphorylated eIF2 is a competitive inhibitor of its own guanine nucleotide exchange factor eIF2B and leads to general inhibition of translation (38, 40). Importantly, regulation of global protein synthesis was also shown to be mediated by phosphatidylinositol 3-kinase (PI3K)/AKT/glycogen synthase kinase 3β (GSK3β) signaling (41) as presented schematically in Fig. 5. GSK3β phosphorylates eIF2B, thus inactivating it and resulting in subsequent inhibition of translation initiation (41). GSK3β, however, is itself negatively regulated by AKT, which phosphorylates and inactivates it (41). Therefore, Ras inhibition by FTS and the consequent inhibition of PI3K/AKT activation that relieves GSK3β will result in phosphorylation and inhibition of eIF2B (see scheme, Fig. 5). This would lead to inhibition of overall translation followed by induction of the stress response pathway. Our analysis shows that FTS indeed induces an increase in ATF3 and ATF4 expression (Fig. 3*B*) as well as in some of their known target genes (Supplementary Table S3). The overall inhibition of translation that seems to be induced by FTS in cancer cells is thus apparently a

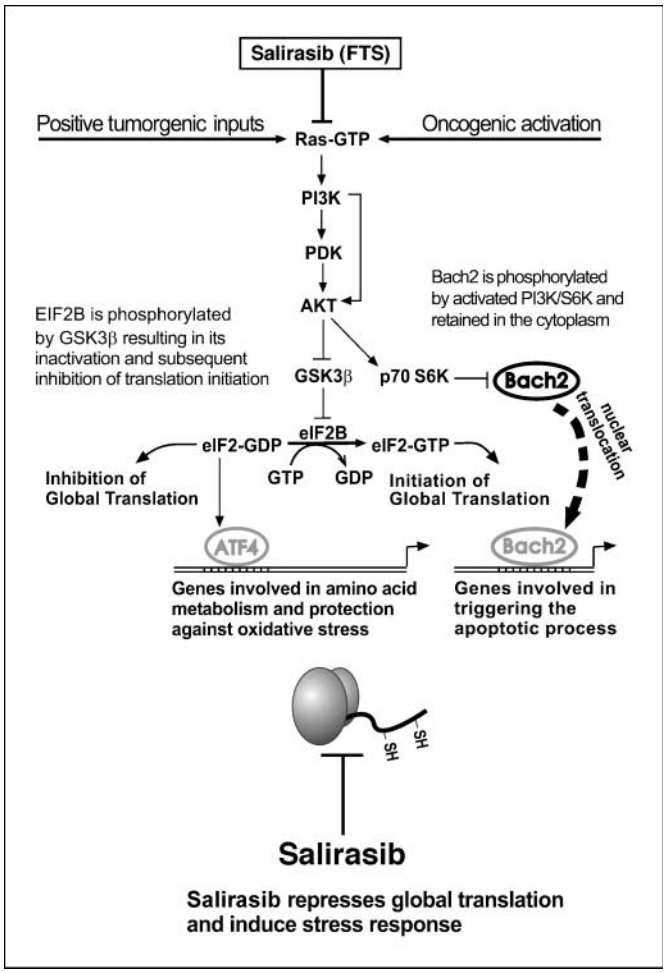

Figure 5. Proposed model for the salirasib-induced repression of the global translation and induction of a response to stress. Ras/PI3K/AKT/GSK3β/eIF2B pathway controlling the initiation of translation pathway (41) and the GSK3β/p70S6K pathway controlling the nuclear translocation of the transcription factor Bach2 (45). Ras inhibition by FTS increases ATF4 levels and nuclear translocation of Bach2.

mirror image of the enhanced overall translation initiation that is induced by oncogenic transformation, especially in highly aggressive tumors (42, 43). For example, constitutive activation of signal transduction pathways (e.g., oncogenic activation of Ras or c-Myc) was shown to lead to continuous up-regulation of key elements of the translational machinery (42). Tumor cells apparently exhibit increased amounts of eIF2α (42) and elevation of global translation initiation (42).

An interesting reported finding was that an increase in the ratio of unphosphorylated to phosphorylated eIF2α facilitates protein synthesis, cell proliferation, and neoplastic transformation (42). Phosphorylation of eIF2α in E2F1$^{-/-}$ murine embryonic fibroblasts (MEF) in response to ER stress was recently shown to be enhanced relative to wild-type MEFs (44). Thus, E2F1 deficiency might lead to a decrease in general translation (44). Because FTS decreases E2F1 in cancer cells (6, 34), this is yet another mechanism through which FTS would block overall translation in such cells.

Enrichment in the group of transcription factors that were up-regulated by FTS was highest for Bach2, suggesting that inhibition of Ras and its pathways might result in up-regulation and/or activation of Bach2 (see scheme, Fig. 5). Bach2 was recently shown to be phosphorylated by PI3K/AKT/p70S6K (45). Phosphorylation of Bach2 by p70S6K leads to retention of Bach2 in the cytoplasm, whereas its dephosphorylation leads to its accumulation in the nucleus, where it induces expression of genes involved in apoptosis (45). It is likely, therefore, that inhibition of the Ras/PI3K/AKT/p70S6K pathway by FTS promoted the increase in Bach2-regulated genes observed in this study (Supplementary Table S4; see scheme, Fig. 5).

Another interesting reported finding was that the transcription and protein expression of Bach2 is negatively regulated by the BCR/ABL oncogene, which also activates Ras and its signaling in BCR/ABL-positive leukemia cells (46). Inhibition of BCR/ABL by Gleevec indeed induced up-regulation of Bach2 at both the transcript and the protein levels. Similarly, both U0126 (MAPK/ERK kinase inhibitor) and LY294002 (PI3K inhibitor) up-regulated Bach2 expression in BCR/ABL-positive lines (46). Other studies showed that Bach2 is induced by oxidative stress (47). As mentioned above, ATF4 is also induced by oxidative stress. Unlike ATF4, however, which enables cells to manage stress conditions as part of the protective response (38, 48), expression of Bach2 is thought to be associated with suppression of the mechanisms that guard cells against oxidative stress (49).

Because FTS seems to increase both ATF4- and Bach2-regulated genes, it is possible that the Ras inhibitor concomitantly causes overall inhibition of translation and stress-associated cell death. The balance between the effects of these two transcription factors might conceivably determine the fate of cancer cell under the stressful conditions apparently imposed on them by FTS. In some cells, the effects of Bach2 will dominate, leading to cell death, whereas in others ATF4 will dominate and protect the cells from death.

In summary, the gene expression profiling data described here provide substantial support for the conclusion that FTS specifically reregulates defective Ras pathways in human tumor cells and strongly suggest that cancer patients with deregulated Ras pathway tumors might benefit from FTS (salirasib) treatment.

Acknowledgments

Received 11/22/2006; revised 1/4/2007; accepted 1/18/2007.

Grant support: The Wolfson Foundation. R. Elkon was supported by an Eshkol Fellowship from the Ministry of Science, Israel.

The costs of publication of this article were defrayed in part by the payment of page charges. This article must therefore be hereby marked *advertisement* in accordance with 18 U.S.C. Section 1734 solely to indicate this fact.

We thank S.R. Smith for editorial assistance.

References

1. Downward J. Targeting RAS signalling pathways in cancer therapy. Nat Rev Cancer 2003;3:11–22.
2. Cox AD, Der CJ. Farnesyltransferase inhibitors: promises and realities. Curr Opin Pharmacol 2002;2:388–93.
3. Blum R, Kloog Y. Tailoring Ras-pathway-inhibitor combinations for cancer therapy. Drug Resist Updat 2005;8:369–80.
4. Kloog Y, Cox AD. RAS inhibitors: potential for cancer therapeutics. Mol Med Today 2000;6:398–402.
5. Blum R, Jacob-Hirsch J, Amariglio N, Rechavi G, Kloog Y. Ras inhibition in glioblastoma down-regulates hypoxia-inducible factor-1α, causing glycolysis shutdown and cell death. Cancer Res 2005;65:999–1006.
6. Yaari S, Jacob-Hirsch J, Amariglio N, et al. Disruption of cooperation between Ras and MycN in human neuroblastoma cells promotes growth arrest. Clin Cancer Res 2005;11:4321–30.
7. Santen RJ, Lynch AR, Neal LR, McPherson RA, Yue W. Farnesylthiosalicylic acid: inhibition of proliferation and enhancement of apoptosis of hormone-dependent breast cancer cells. Anticancer Drugs 2006;17:33–40.
8. Halaschek-Wiener J, Wacheck V, Kloog Y, Jansen B. Ras inhibition leads to transcriptional activation of p53 and down-regulation of Mdm2: two mechanisms that cooperatively increase p53 function in colon cancer cells. Cell Signal 2004;16:1319–27.
9. Bild AH, Yao G, Chang JT, et al. Oncogenic pathway signatures in human cancers as a guide to targeted therapies. Nature 2006;439:353–7.
10. Segal E, Friedman N, Koller D, Regev A. A module map showing conditional activity of expression modules in cancer. Nat Genet 2004;36:1090–8.
11. Potti A, Dressman HK, Bild A, et al. Genomic signatures to guide the use of chemotherapeutics. Nat Med 2006;12:1294–300.
12. Sears RC, Nevins JR. Signaling networks that link cell proliferation and cell fate. J Biol Chem 2002;277:11617–20.
13. Elkon R, Linhart C, Sharan R, Shamir R, Shiloh Y. Genome-wide *in silico* identification of transcriptional regulators controlling the cell cycle in human cells. Genome Res 2003;13:773–80.
14. Shamir R, Maron-Katz A, Tanay A, et al. EXPANDER—an integrative program suite for microarray data analysis. BMC Bioinformatics 2005;6:232.
15. Sharan R, Shamir R. CLICK: a clustering algorithm with applications to gene expression analysis. Proc Int Conf Intell Syst Mol Biol 2000;8:307–16.
16. Blum R, Jacob-Hirsch J, Rechavi G, Kloog Y. Suppression of survivin expression in glioblastoma cells by the Ras inhibitor farnesylthiosalicylic acid promotes caspase-dependent apoptosis. Mol Cancer Ther 2006;5:2337–47.
17. Tong T, Ji J, Jin S, et al. Gadd45a expression induces Bim dissociation from the cytoskeleton and translocation to mitochondria. Mol Cell Biol 2005;25:4488–500.
18. Blais JD, Filipenko V, Bi M, et al. Activating transcription factor 4 is translationally regulated by hypoxic stress. Mol Cell Biol 2004;24:7469–82.
19. Yoon SO, Shin S, Mercurio AM. Ras stimulation of E2F activity and a consequent E2F regulation of integrin $\alpha_6\beta_4$ promote the invasion of breast carcinoma cells. Cancer Res 2006;66:6288–95.
20. Berkovich E, Ginsberg D. Ras induces elevation of E2F-1 mRNA levels. J Biol Chem 2001;276:42851–6.
21. Gu Z, Kuntz-Simon G, Rommelaere J, Cornelis J. Oncogenic transformation-dependent expression of a transcription factor NF-Y subunit. Mol Carcinog 1999;24:294–9.
22. Pruitt K, Pestell RG, Der CJ. Ras inactivation of the retinoblastoma pathway by distinct mechanisms in NIH 3T3 fibroblast and RIE-1 epithelial cells. J Biol Chem 2000;275:40916–24.
23. Johnson DG, Cress WD, Jakoi L, Nevins JR. Oncogenic capacity of the E2F1 gene. Proc Natl Acad Sci U S A 1994;91:12823–7.
24. Zhu W, Giangrande PH, Nevins JR. E2Fs link the control of G_1/S and G_2/M transcription. EMBO J 2004;23:4615–26.
25. Salsi V, Caretti G, Wasner M, et al. Interactions between p300 and multiple NF-Y trimers govern cyclin B2 promoter function. J Biol Chem 2003;278:6642–50.
26. Fan J, Bertino JR. K-ras modulates the cell cycle via both positive and negative regulatory pathways. Oncogene 1997;14:2595–607.
27. Hai T, Wolfgang CD, Marsee DK, Allen AE, Sivaprasad U. ATF3 and stress responses. Gene Expr 1999;7:321–35.
28. Bogoyevitch MA, Gillespie-Brown J, Ketterman AJ, et al. Stimulation of the stress-activated mitogen-activated protein kinase subfamilies in perfused heart. p38/RK mitogen-activated protein kinases and c-Jun N-terminal kinases are activated by ischemia/reperfusion. Circ Res 1996;79:162–73.
29. Rhodes DR, Yu J, Shanker K, et al. Large-scale meta-analysis of cancer microarray data identifies common transcriptional profiles of neoplastic transformation and progression. Proc Natl Acad Sci U S A 2004;101:9309–14.
30. Liang Y, Diehn M, Watson N, et al. Gene expression profiling reveals molecularly and clinically distinct subtypes of glioblastoma multiforme. Proc Natl Acad Sci U S A 2005;102:5814–9.

31. Sharan R, Maron-Katz A, Shamir R. CLICK and EXPANDER: a system for clustering and visualizing gene expression data. Bioinformatics 2003;19:1787–99.

32. Aktas H, Cai H, Cooper GM. Ras links growth factor signaling to the cell cycle machinery via regulation of cyclin D1 and the Cdk inhibitor p27KIP1. Mol Cell Biol 1997;17:3850–7.

33. Alabert C, Rogers L, Kahn L, et al. Cell type-dependent control of NF-Y activity by TGF-β. Oncogene 2006;25:3387–96.

34. Blum R, Nakdimon I, Goldberg L, et al. E2F1 identified by promoter and biochemical analysis as a central target of glioblastoma cell-cycle arrest in response to Ras inhibition. Int J Cancer 2006;119:527–38.

35. Scarpulla RC. Nuclear activators and coactivators in mammalian mitochondrial biogenesis. Biochim Biophys Acta 2002;1576:1–14.

36. Zhang H, Liu H, Iles KE, et al. 4-Hydroxynonenal induces rat γ-glutamyl transpeptidase through mitogen-activated protein kinase-mediated electrophile response element/nuclear factor erythroid 2-related factor 2 signaling. Am J Respir Cell Mol Biol 2006;34:174–81.

37. Cam H, Balciunaite E, Blais A, et al. A common set of gene regulatory networks links metabolism and growth inhibition. Mol Cell 2004;16:399–411.

38. Harding HP, Novoa I, Zhang Y, et al. Regulated translation initiation controls stress-induced gene expression in mammalian cells. Mol Cell 2000;6:1099–108.

39. Novoa I, Zeng H, Harding HP, Ron D. Feedback inhibition of the unfolded protein response by GADD34-mediated dephosphorylation of eIF2α. J Cell Biol 2001;153:1011–22.

40. Ron D. Translational control in the endoplasmic reticulum stress response. J Clin Invest 2002;110:1383–8.

41. Welsh GI, Miller CM, Loughlin AJ, Price NT, Proud CG. Regulation of eukaryotic initiation factor eIF2B: glycogen synthase kinase-3 phosphorylates a conserved serine which undergoes dephosphorylation in response to insulin. FEBS Lett 1998;421:125–30.

42. Rosenwald IB. The role of translation in neoplastic transformation from a pathologist's point of view. Oncogene 2004;23:3230–47.

43. Meric F, Hunt KK. Translation initiation in cancer: a novel target for therapy. Mol Cancer Ther 2002;1:971–9.

44. Park KM, Kim DJ, Paik SG, Kim SJ, Yeom YI. Role of E2F1 in endoplasmic reticulum stress signaling. Mol Cell 2006;21:356–9.

45. Yoshida C, Yoshida F, Sears D, et al. Bcr-Abl signaling through the PI-3/S6 kinase pathway inhibits nuclear translocation of the transcription factor Bach2, which represses the anti-apoptotic factor heme oxygenase-1. Blood 2007;109:1211–9.

46. Vieira SA, Deininger MW, Sorour A, et al. Transcription factor BACH2 is transcriptionally regulated by the BCR/ABL oncogene. Genes Chromosomes Cancer 2001;32:353–63.

47. Muto A, Tashiro S, Tsuchiya H, et al. Activation of Maf/AP-1 repressor Bach2 by oxidative stress promotes apoptosis and its interaction with promyelocytic leukemia nuclear bodies. J Biol Chem 2002;277:20724–33.

48. Vattem KM, Wek RC. Reinitiation involving upstream ORFs regulates ATF4 mRNA translation in mammalian cells. Proc Natl Acad Sci U S A 2004;101:11269–74.

49. Kamio T, Toki T, Kanezaki R, et al. B-cell-specific transcription factor BACH2 modifies the cytotoxic effects of anticancer drugs. Blood 2003;102:3317–22.